Vorlesung 11 STM

Wednesday, 13. July 2022 13:57

4. Spins on Surfaces (SOS)

- Molecular spin qubits: ⊕ great Q-properties (spin engineering)
  very stable devices
  ⊖ no spatial information + control

Idea: Use a technique that can image molecules and allow devices engineering

⇒ Scanning Tunneling Microscopy STM

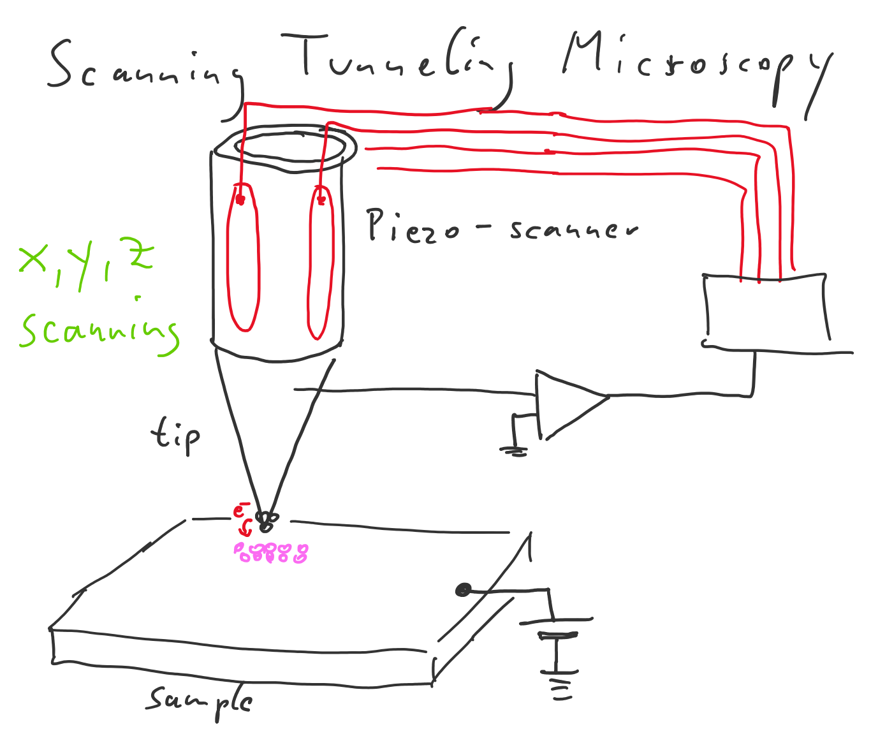

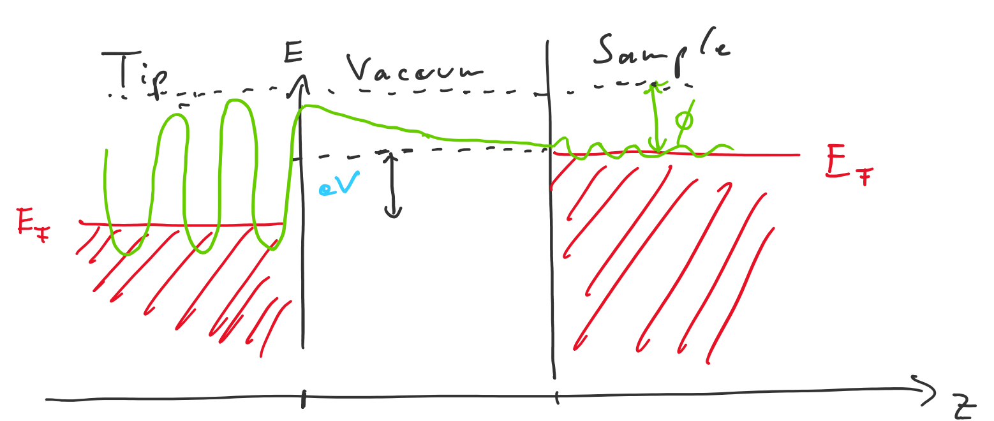

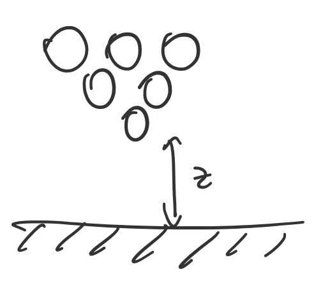

wave fct.:

$$\Psi(z) = \Psi(0)\cdot\exp[-kz]$$

transmission

$$T = \frac{I(z)}{I(0)} = \exp[-2kz]$$

$$k = \frac{\sqrt{2m\phi}}{\hbar}$$

- tunnel current $I(z)$ is very sensitive to distance z

$$I(z) \sim pA - nA$$

4.1 Local atomic spins on a surface

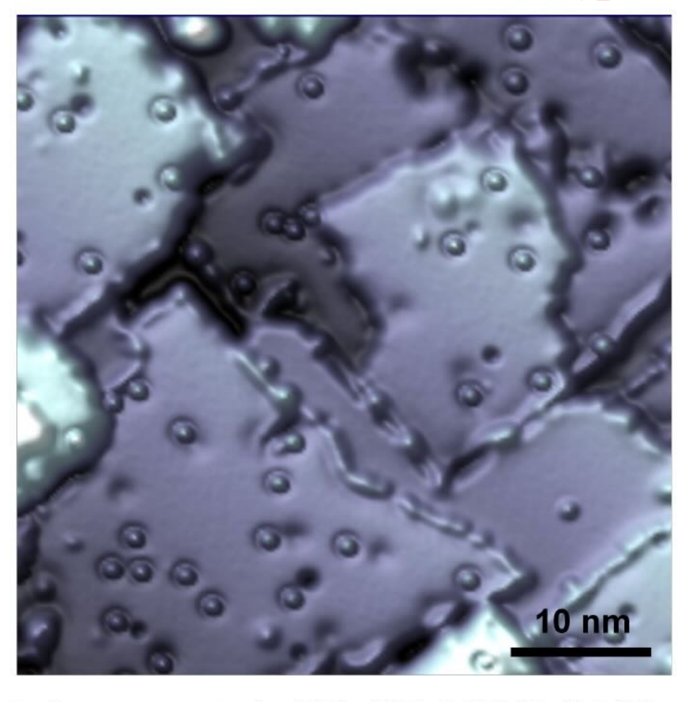

S. Baumann et al., *PRL* **115**, *237202* (2015)

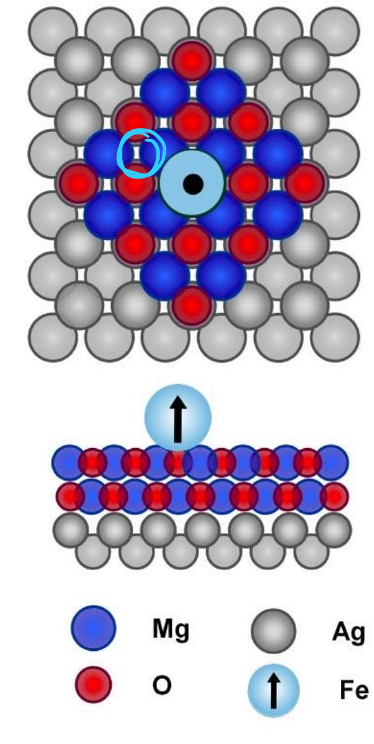

Spin sensitivity

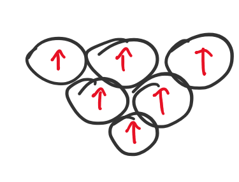

- Insolator to decouple the SOS from strong interaction with substrate (0.5 - 1 nm thick)

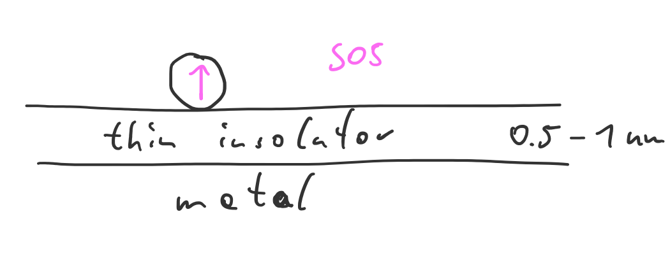

Readout

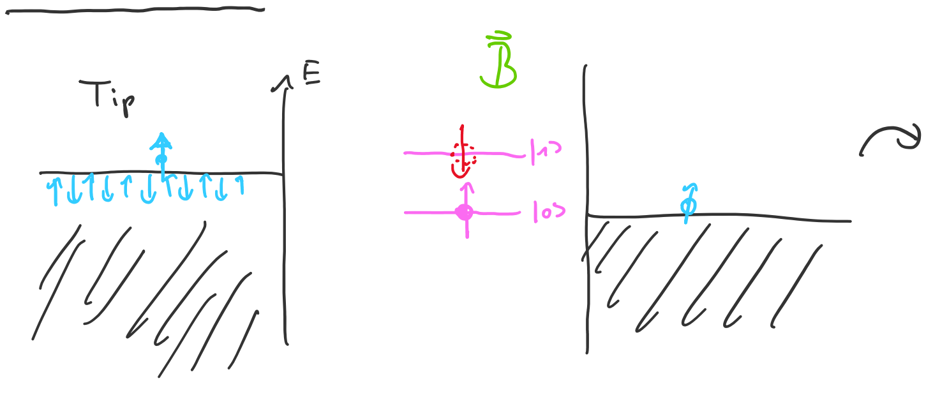

↷ spin dependent tunneling

- elastic or inelastic tunneling path possible
  → I depends on - spin of tunneling e⁻
  - spin on the surface

  → using a magnetic tip to increase the tunneling of one spin direction
  ⇒ spin-polarized tunneling

$$\Rightarrow I = g(\underset{\uparrow\ \text{local spin}}{m})\cdot V = (P_0\,\sigma_0 + P_1\,\sigma_1)\cdot V$$

conductances of SOS 0 or 1 (σ_0, σ_1)

Probability of SOS in 0 or 1 (P_0, P_1)

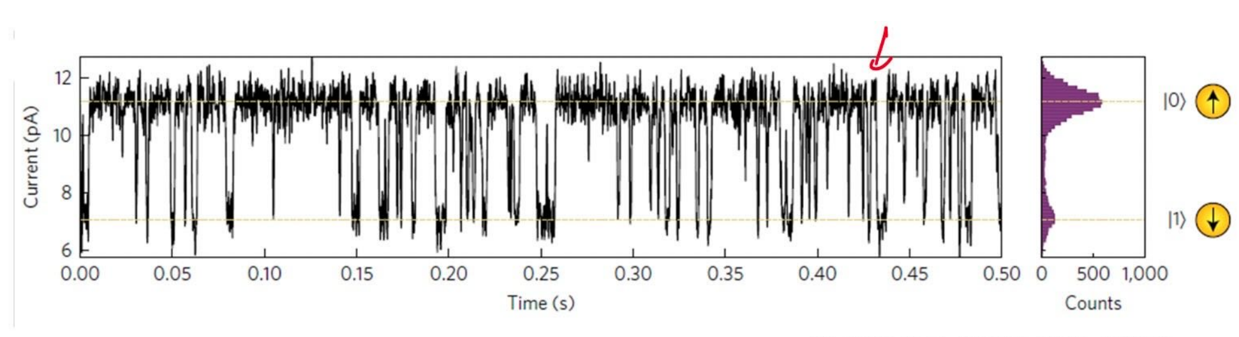

W. Paul et al., Nature Phys. (2017)

Spin Hamiltonians

- molecular magnets have a ligand field
- atoms on surfaces see a crystal field of the surface

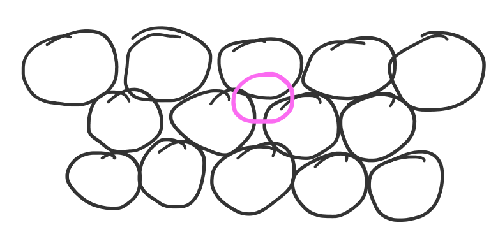

Spin resonance

$$-\tfrac{1}{2}\to\tfrac{1}{2}\ \hat{=}\ 1$$

$$S = \frac{1}{2} \qquad hf_0 = g\mu_B B\,\Delta m_s \approx 2\mu_B B = 28\,\frac{GHz}{T}\cdot B$$

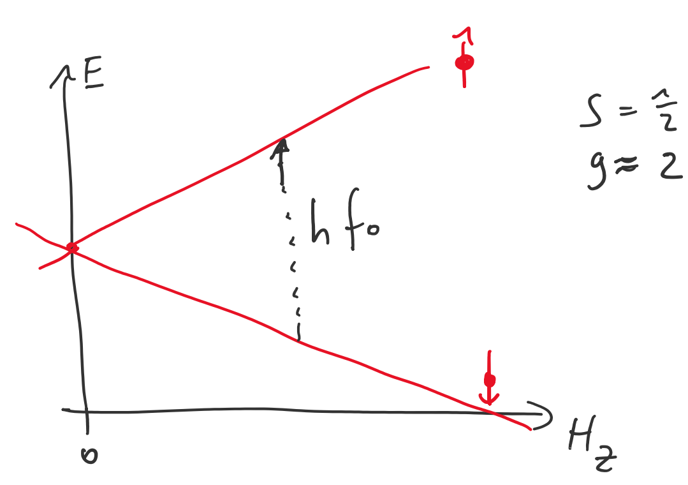

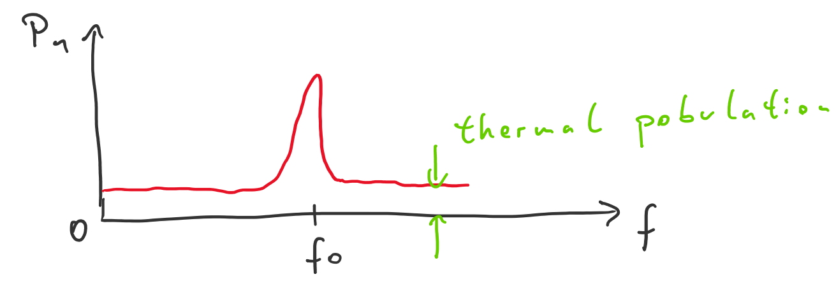

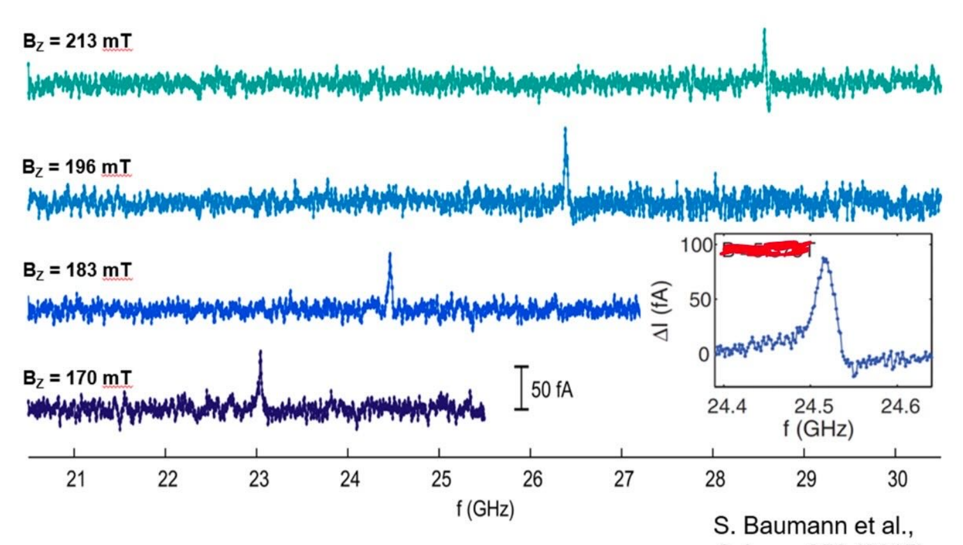

S. Baumann et al., *Science* **350** (2015)

4.2 Spin excitation

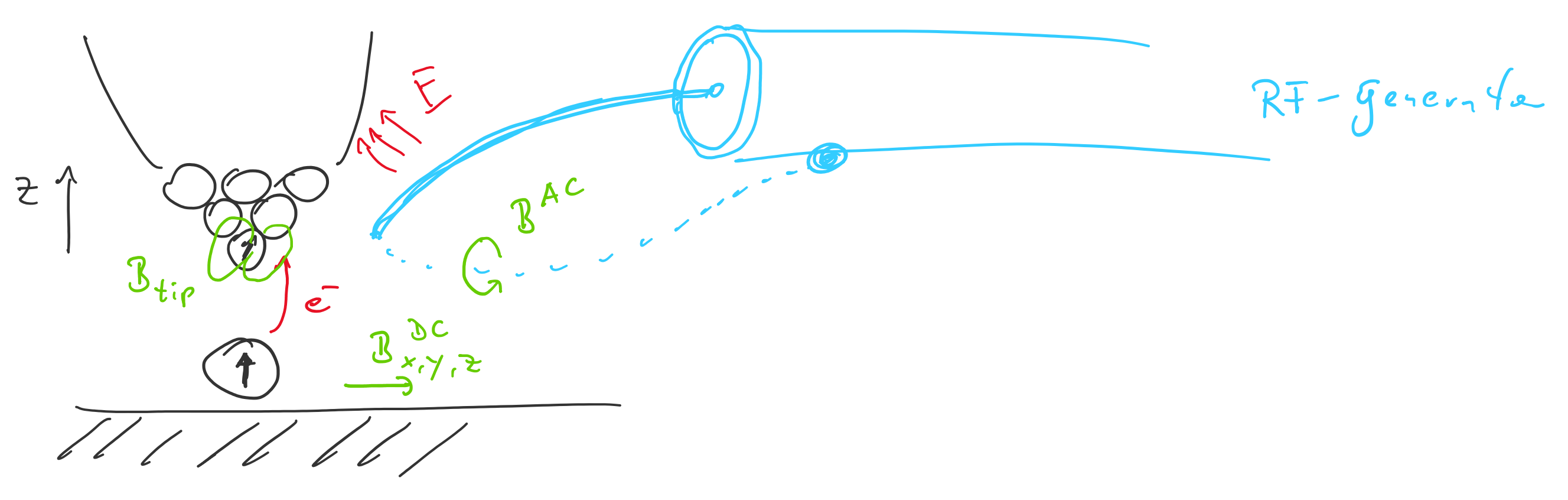

- local enhancement via electric field
- B_{tip} - magnetic dipole interaction
  - exchange interaction

$$H = J\cdot\vec{S}_{SOS}\,\underbrace{\vec{S}_{Tip}}_{B_{tip}} = \underbrace{J_0\exp\left(-\frac{z}{d_{exchange}}\right)}_{\text{wavefunction overlap}}\cdot\vec{S}_{SOS}\,\vec{S}_{Tip}$$

$$\Delta B_{tip}(z) = \frac{\partial B_{tip}}{\partial z}\,\Delta z\cdot\sin(\varphi)$$

$$\simeq -\frac{B_{tip}}{d_{ex}}\,\Delta z\,\sin(\varphi)$$

- vertical displacement Δz

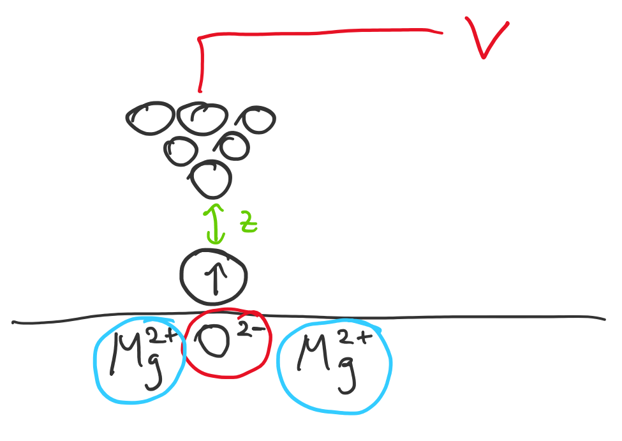

- electric field
  $E = \frac{V}{z}$ $\left(\sim 10^7 - 10^8\,\frac{V}{m}\right)$
- inhomogeneous charge distribution
- stiffness of atomic bonds

$$F_{electric\,field} = F_{spring}$$

V_{RF} ~ shaking of atom by the electric field
~ modulation of crystal field

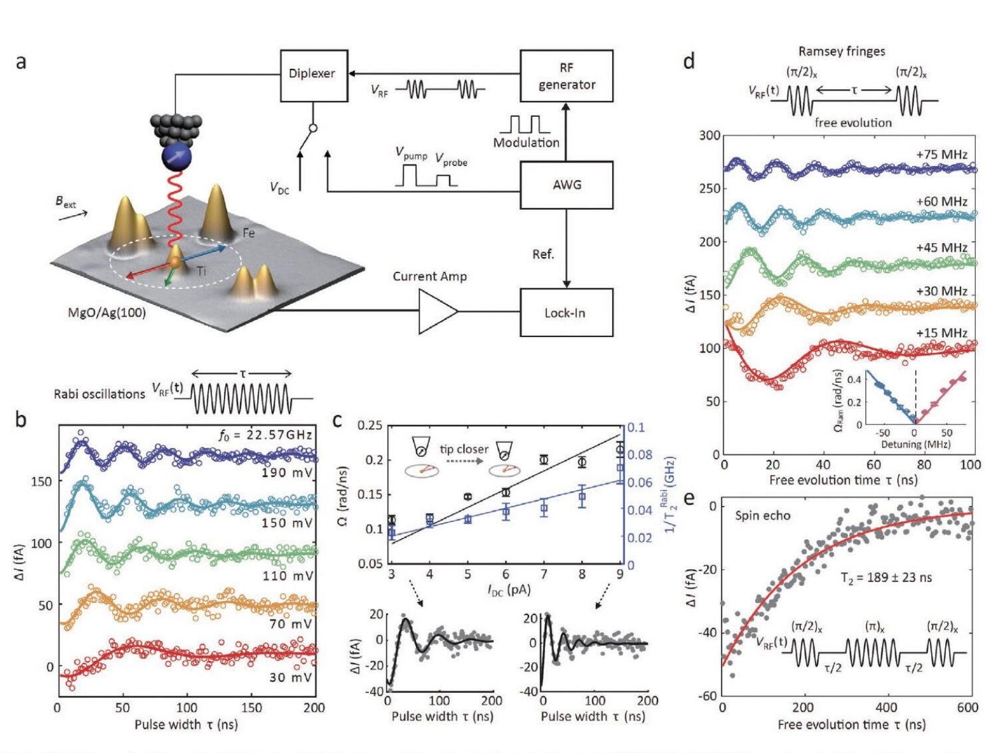

Figure 10. Coherent spin manipulation of a single Ti atom. a) Experimental setup for pulsed ESR-STM. The STM is equipped with an RF generator and an AWG. A sequence of RF and DC pulses are delivered to an oxygen-site Ti atom on MgO/Ag(100) via the STM tip. b) Rabi oscillations of the Ti spin at different RF powers (V_{RF}). c) Rabi rates and coherence times measured at different tip-atom separations. d) Ramsey fringe measurement of the Ti spin. e) Hahn echo measurements of the Ti spin, yielding $T_2 = 189 \pm 23$ ns. Reproduced with permission.[30] Copyright 2019, AAAS.

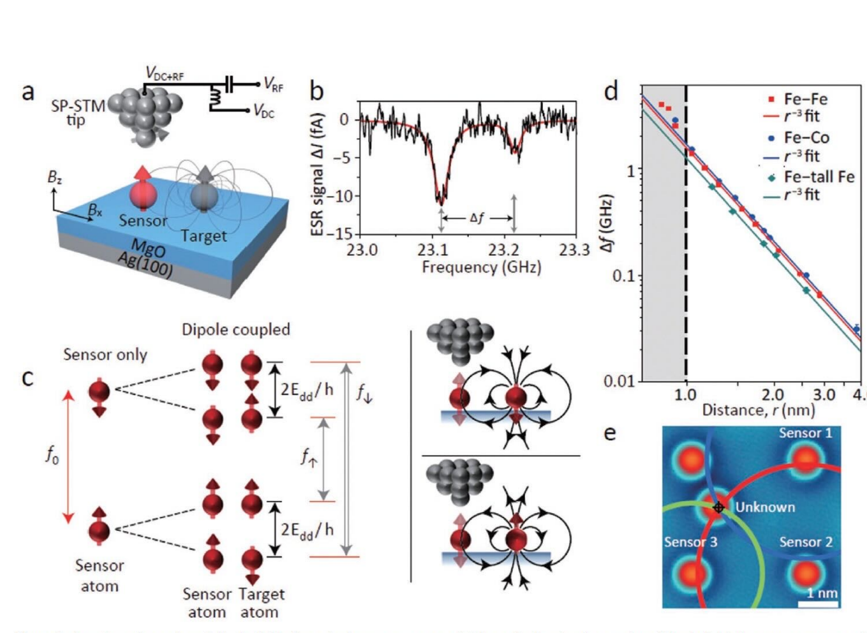

Figure 6. Atomic-scale sensing of dipolar fields from single-atom magnets. a) Schematic showing the sensing of dipole fields from a target atom using a sensor spin. b) ESR spectrum obtained from an Fe atom (sensor) separated by 2.46 nm from another Fe atom (target). c) Schematic energy diagram of the sensor atom under the influence of the dipole fields of the target atom. Two ESR peaks in (b) correspond to the two transitions marked by grey arrows in (c). The Zeeman energy of the target spin is not included in the energy level diagram. d) ESR splitting as a function of atomic separations for pairs of Fe-Fe, Fe-Co, and Fe-"tall" Fe. The observed r^{-3}-distance dependence indicates that dipole–dipole interactions dominate at these separations, while deviations in the grey area (with r less than 1 nm) result from additional exchange interactions. The magnetic moments extracted from the fits are $5.44 \pm 0.03\,\mu_B$ for Fe, $5.88 \pm 0.06\,\mu_B$ for Co, and $4.35 \pm 0.08\,\mu_B$ for "tall" Fe. e) An STM image of five Fe atoms used in "nano-GPS." Through trilateration using three sensor atoms, the location and the magnetic moment of a target, unknown atom can be determined. Reproduced with permission.[42] Copyright 2017, Springer Nature.

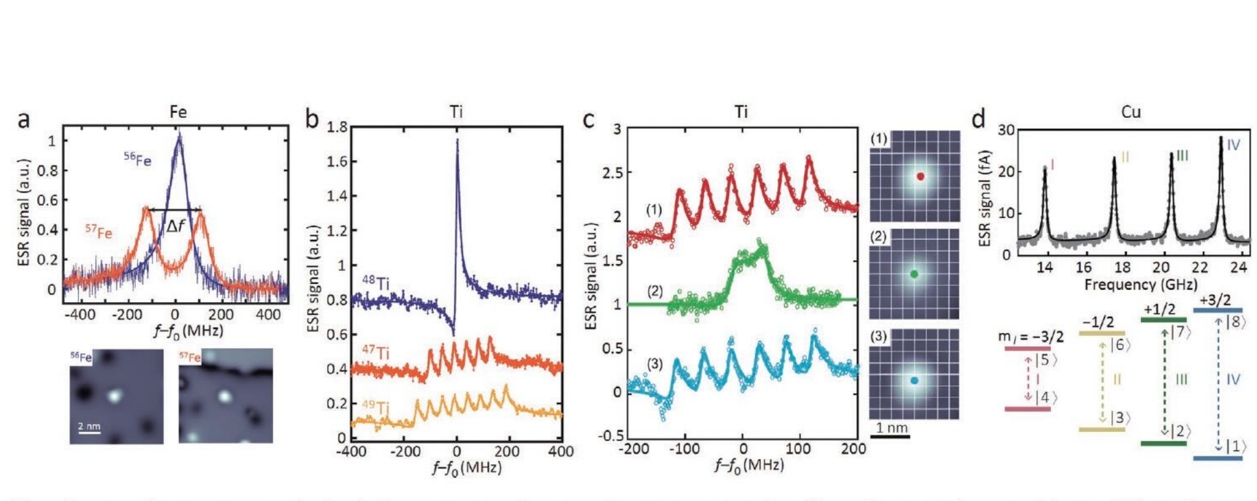

Figure 7. Hyperfine interactions of individual atoms on a surface. a) ESR spectra measured on ^{56}Fe with zero nuclear spin (blue) and ^{57}Fe with $I = 1/2$ (orange). The bottom panels show STM images of ^{56}Fe and ^{57}Fe. b) ESR spectra measured on bridge-site Ti atoms with different nuclear spins. A single ESR peak was observed on ^{48}Ti that carries no nuclear spin, while six and eight ESR peaks were seen for ^{47}Ti ($I = 5/2$) and ^{49}Ti ($I = 7/2$), respectively. c) Binding-site-dependent ESR spectra of the same ^{47}Ti atom moved by lateral atom manipulation. Right: STM images showing the Ti binding sites where the spectra on the left are taken. The Ti atom was changed from 1) a bridge site to 2) an oxygen site then back to 3) a bridge site. The interception points of the grid correspond to oxygen sites of MgO. d) ESR spectrum of ^{65}Cu ($I = 3/2$) on MgO. Lower panel: Schematic energy diagram of Cu with $S = 1/2$ and $I = 3/2$. (a–c) reproduced with permission.[45] Copyright 2018, AAAS. (d) reproduced with permission.[35] Copyright 2018, Springer Nature.